AAS 16-228

NAVIGATION AND STATISTICAL DELTA-V ANALYSIS FOR DOUBLE-SATELLITE-AIDED CAPTURE AT JUPITER

Alfred E. Lynam*, Alan M. Didion†

Double-satellite-aided capture substantially reduces a mission's deterministic ΔV by using gravity assists of two of Jupiter's massive Galilean moons in addition to a Jupiter orbit insertion (JOI) maneuver. The statistical ΔV savings of double-satellite-aided capture vs. single-satellite-aided capture is more difficult to characterize because they are strongly dependent on the specifics of navigation technologies and methodologies. In this paper, we estimate the statistical ΔV required to execute Ganymede-Io-JOI (GIJ), Ganymede-Europa-JOI (GEJ), and Callisto-Ganymede-JOI (CGJ) double-satellite-aided capture using two different navigation assumptions with two different degrees of conservatism. Results show that updating the navigation solution and including a trajectory correction maneuver in between flybys results in a statistical ΔV of around 10 m/s (in addition to the deterministic JOI ΔV). The more conservative scenarios with no corrections until the JOI cleanup maneuver days later have higher statistical ΔV's, but the CGJ scenario is the only one that has a small risk (0.265%) of crashing into a moon.

INTRODUCTION

Satellite-aided capture involves the use of one or more gravity assists of planetary moons in order to reduce or eliminate the ΔV requirements for capture into planetary orbits.[1−6] The technique is especially useful in the Jupiter system due to the large masses of the Galilean moons of Jupiter; Callisto,[7] Ganymede,[8] Europa,[9] and Io[10] have gravitational parameters of 7179.289, 9887.834, 3202.739, and 5959.916 km^3/s^2, respectively. The Galileo mission[11,12] used a single-satellite-aided capture with a gravity assist of Io to reduce its JOI ΔV requirements for capture into Jupiter orbit.

Double-satellite-aided capture[1,2,4,13–19] and triple-satellite-aided capture[20−25] have also been investigated. Table 1 lists the deterministic ΔV costs for different types of Jupiter capture sequences at various perijoves.

While Table 1 shows that double- and triple-satellite-aided capture sequences can save 100's of meters per second of deterministic ΔV versus single-satellite-aided capture, it does not provide any insight into the statistical ΔV required to successfully navigate them. While deterministic trajectory design using ΔV as a primary figure of merit is usually abstract enough that spacecraft design and technology choices can be ignored, even a preliminary analysis of spacecraft navigation requires

*Assistant Professor, Mechanical and Aerospace Engineering Department, West Virginia University, ESB, Evansdale Dr. Room 931, Morgantown, WV 26506-6106. Member AIAA. Member AAS.
†Graduate Student, Mechanical and Aerospace Engineering Department, West Virginia University, ESB, Evansdale Dr. Room 931, Morgantown, WV 26506-6106.

Table 1. Perijoves and ΔV costs required to capture into a 200-day orbit for unaided capture and single-, double-, triple-, and quadruple-satellite-aided capture sequences.

Perijoves	13 R_{J}	9 R_{J}	5 R_{J}	1.01 R_{J}
Unaided ΔV	1317 m/s	1101 m/s	825 m/s	371 m/s
Single ΔV	863 m/s	771 m/s	556 m/s	308 m/s
Double ΔV	498 m/s	529 m/s	330 m/s	228 m/s
Triple ΔV	—	330 m/s	202 m/s	190 m/s
Quadruple ΔV	—	—	—	159 m/s

a number of assumptions about the available technology. Radiometric navigation can estimate the Earth-centered position and velocity of a spacecraft to high precision.[26,27] However, knowledge of the position and velocity of the spacecraft with respect to Jupiter and its moons is far more important when attempting multiple-satellite-aided capture. Even with an excellent Earth-centered navigation solution, errors in the *a priori* ephemerides of Jupiter and its moons can substantially degrade the navigation solution with respect to the Jupiter system bodies. The errors in the ephemeris of a moon can only be corrected via radiometric navigation after the spacecraft flies by that moon.

Two papers have analyzed multiple-satellite-aided capture from a navigational perspective: Lynam and Longuski[28] and Didion and Lynam.[29] Lynam and Longuski showed that double-satellite-aided capture was safe to navigate in terms of avoiding collisions with Galilean moons, but did not analyze the statistical ΔV required to correct the trajectories afterward. They also showed that triple-satellite-aided captures would require trajectory correction maneuvers (TCMs) between flybys in order to avoid collisions with the Galilean moons. Didion and Lynam[29] performed a Monte Carlo simulation of the navigation of a particular Callisto-Io-JOI-Ganymede triple-satellite-aided capture sequence. They assumed the use of an autonomous navigation system that could execute TCMs at the periapsides of the flybys. They modeled a TCM at the periapsis of the first flyby (of Callisto) that targets the second flyby (of Io). After the second flyby of Io, the JOI maneuver is re-targeted to target the third flyby (of Ganymede). Three days later, a JOI cleanup maneuver is used to target the nominal apojove position.

This paper uses a similar Monte Carlo simulation setup to Didion and Lynam,[29] but we investigate double-satellite-aided capture trajectories instead of triple-satellite-aided capture. We also investigate single-satellite-aided capture purely for comparison purposes. We use integrated GMAT trajectories from Lynam[30] as nominal trajectories for the statistical ΔV analysis. Similarly to Lynam, we are only interested in double-satellite-aided capture trajectories that have both flybys before JOI—Callisto-Ganymede-JOI (CGJ), Ganymede-Europa-JOI (GEJ), and Ganymede-Io-JOI (GIJ) sequences. Double-satellite-aided capture sequences that have flybys after JOI would suffer from increased errors and collision risks due to the JOI dispersion, so they are not considered here.

In order to characterize the double-satellite-aided capture navigation problem as thoroughly as possible, we perform several different Monte Carlo simulations for each nominal trajectory. The first category of Monte Carlo simulation is the most conservative; no TCMs are allowed in between flybys and the JOI maneuver is not allowed to be re-targeted. A JOI cleanup maneuver is allowed 1, 2, or 3 days (we do simulations for all three scenarios) after the JOI maneuver to correct the trajectory. The second category of Monte Carlo simulation is less conservative than the first, but

Table 2. GMAT double-satellite-aided capture solutions from Lynam.[30]

Solution	Launch	Launch C_3	Arrival	$m_{\text{post-JOI}}$	Perijove
GIJ	6/22/2022	84.0 km^2/s^2	1/20/2025	3958 kg	5.44 R_J
GEJ	6/22/2022	83.4 km^2/s^2	4/9/2025	3274 kg	8.69 R_J
CGJ	7/27/2023	83.2 km^2/s^2	10/19/2026	3669 kg	8.57 R_J

still doable with only ground-based radiometric navigation. A TCM is allowed six hours after the first flyby, and the JOI maneuver is re-targeted. A JOI cleanup maneuver is still added 1, 2, or 3 days after the JOI maneuver. This strategy would require continuous Deep Space Network tracking during and after the first flyby, a "canned" maneuver prepared, and rapid decision making on the ground. In the unlikely event that this strategy were to fail, the first strategy would serve as an automatic fallback option.

METHODOLOGY

Nominal Trajectories

The nominal trajectories for the double-satellite-aided capture trajectories were developed in GMAT by Lynam.[30] The trajectories assumed that the SLS (Space Launch System) Block I would be used to inject the spacecraft into a direct transfer from Earth to Jupiter with a deep space maneuver. The spacecraft would then capture into Jupiter orbit using a double-satellite-aided capture sequence. Lynam found 6 GIJ and 2 GEJ trajectories in the 2022 launch window, and 8 GIJ and 7 CGJ trajectories in the 2023 launch window. One of each sequence was chosen as a nominal trajectory for the navigation analysis. Table 2 summarizes the 3 trajectories that were chosen from the trajectories in Tables 2 and 3 of Lynam.[30]

As noted by Lynam,[30] there were not any particularly good GEJ trajectories during the 2022 and 2023 launch windows, so the least bad trajectory was chosen instead. The CGJ solutions had good mass properties but perijoves that were lower than those of some of the other windows. The CGJ solution with the highest perijove in the 2023 window was chosen. The GIJ solution in the 2022 window with the best mass properties and a reasonably high perijove was chosen.

Separate nominal trajectories for single-satellite-aided captures were developed in GMAT for comparison purposes. The nominal Io-Jupiter (IJ) capture was reconstructed in GMAT from data available from the Jupiter Europa Orbiter (JEO) mission study.[31] The nominal Ganymede-Jupiter (GJ) capture was reconstructed in GMAT from data available from the nominal Europa Mission.[32]

For the purposes of this paper, each of the nominal trajectories is initialized about 3 days before its first flyby. Thus, initial states were extracted from the GMAT trajectories to be used as initial states for the MATLAB navigation model. The initial epochs and states for the 5 nominal trajectories are tabulated in Table 3.

Navigation Error Estimates

As mentioned in the introduction, the navigation model used in this paper is very similar to that used by Didion and Lynam.[29] The 7-body dynamical model integrates the spacecraft's trajectory

Table 3. Initial epochs and states for 5 nominal trajectories. Jupiter-centered, ecliptic J2000 coordinates are used.

	Epoch	X, km	Y, km	Z, km	Vx, km/s	Vy, km/s	Vz, km/s
GIJ	1/17/2025 1:46:39	-3973976	-448184	-81509	9.6092	-1.6142	0.1007
GEJ	4/5/2025 21:29:43	-4010853	-492056	-109077	9.7851	-2.2064	0.1558
CGJ	10/16/2026 18:13:48	-2697639	-2919406	-107698	8.8983	4.3226	0.1654
IJ	12/18/2025 7:53:47	-2344102	-2501827	68960	8.7934	5.1842	-0.2226
GJ	3/1/2025 4:17:43	-3996068	-932363	131841	9.5775	-1.7597	-0.4972

using 6 gravitating bodies with Jupiter as the central body and the Sun and four Galilean moons as perturbing bodies. A state error transition matrix is integrated simultaneously with the spacecraft's trajectory. The state transition matrix allows the mapping of errors in the initial state of the spacecraft and the ephemerides of the Galilean moons into spacecraft errors at any other time in the trajectory.

The 1σ initial position error estimates are based on the following reasoning. We assume that the errors due to uncertainty in Jupiter's position will be reduced to 1 km in each direction as a result of navigation and radio science of the Juno mission, which will arrive at Jupiter in July 2016 before any of the nominal trajectories. The knowledge errors of the spacecraft with respect to Earth in the radiometric ranging direction are on the order of tens of meters, so we neglect them in this analysis. The errors in the cross-track and out-of-plane directions are 2 km, which is based on conservative estimates of the Delta-Differential One-Way Ranging (Delta-DOR) capacity of radiometric navigation in the 2020's.[33]

Jupiter is approximately in the y-direction from Earth in 2025 and 2026 in terms of the ecliptic coordinates we are using, so we assume that y is the range direction, x is the cross-track direction, and z is the out-of-plane direction. Adding the Jupiter position error estimates to the Delta-DOR errors gives 1σ initial position error estimates of 3 km, 1 km, and 3 km in the x, y, and z directions, respectively. (Technically, the Jupiter position error and the Delta-DOR error are uncorrelated, so adding the errors rather than using two separate errors is another conservative assumption.)

The 1σ initial velocity error estimates are 1 mm/s in each direction. This estimate is also conservative and based on the accuracy of Doppler radiometric data and ranging/Delta-DOR data collected over time. The 1σ errors on the ephemerides of the 4 Galilean moons are 5 km in the radial (R), downtrack (T), and out-of-plane (N) directions.[34] After a flyby, we assume that radiometric navigation is sufficient to reduce the 1σ spacecraft position and ephemeris errors (of that particular moon) to 0.1 km in each direction. The ephemerides of the other moons cannot be corrected until after a flyby is done of them. The 1σ error estimates are tabulated in Table 4.

The maneuver execution errors for the JOI maneuvers and the TCM before the second flyby (in scenarios that use that TCM) are based on the Cassini maneuver execution error models.[35] The JOI maneuver inconsistently uses the 2000 model of the Cassini Main Engine Assembly (MEA) for its magnitude component and the 2007-2 model of the MEA for the pointing component. (The different models were used accidentally, but the magnitude component is the one that causes the most downstream error so the model should be conservative.) The TCM before the second flyby uses

Table 4. 1σ **initial state and ephemeris errors for nominal trajectories.**

	Before Flyby	After Flyby
δX, km	3.0	0.1
δY, km	1.0	0.1
δZ, km	3.0	0.1
δVx, mm/s	1.0	1.0
δVy, mm/s	1.0	1.0
δVz, mm/s	1.0	1.0
Moon δR, km	5.0	0.1
Moon δT, km	5.0	0.1
Moon δN, km	5.0	0.1

Table 5. Maneuver execution errors. The magnitude values for the Cassini MEA model use the 2000 model and the pointing values use the 2007-2 model.

Component	2000/2007-2 Cassini MEA model	2007-2 Cassini RCS model
Magnitude Proportional	0.2%	1.2%
Magnitude Fixed	10 mm/s	0.8 mm/s
Pointing Proportional	0.6 mrad	5.5 mrad
Pointing Fixed	3.0 mm/s	0 mm/s

the equivalent of the 2007-2 model of the Cassini Reaction Control System (RCS). The maneuver execution errors in the JOI cleanup maneuver and the velocity mismatch at apojove are neglected since we are primarily interested in dealing with the errors caused by the double-satellite-aided capture sequence.

The Gates[36] maneuver execution error model is used with the error values from the Cassini models. The error in the magnitude direction of the maneuvers is different from the errors in the two pointing directions. Each of the two pointing directions have equal 1σ values, but they are uncorrelated. The 1σ values for the magnitude and pointing directions have two components: a proportional component that is multiplied by the nominal magnitude of the maneuver and a fixed component that is constant for any maneuver size. (The fixed component is squared and added to the square of the product of the maneuver magnitude and the proportional component to get the variance. The 1σ error values are the square root of the variance.) The proportional and fixed components for the magnitude and pointing errors for both the 2000 MEA model and the 2007-1 RCS model are given in Table 5.

Navigation Models

In this paper, we perform Monte Carlo analyses on each of the 5 nominal trajectories. For the single-satellite-aided capture trajectories, the spacecraft is first propagated to its flyby. We model the error on the flyby by multiplying the state transition matrix by initial state errors that are sampled from a Gaussian distribution with a standard deviation equal to the 1σ values given in the previous section. The trajectory is then propagated to perijove, where the error is updated again via state transition matrix. The Cassini MEA maneuver error model is used to model the error on the JOI maneuver. The perturbed trajectory is propagated 1, 2, or 3 days after the JOI maneuver before a JOI cleanup maneuver is used to target the nominal apojove position of the approximately 200 day capture orbit. The difference between the nominal apojove velocity and the actual velocity of the perturbed trajectory is considered to be a third ΔV.

Ballistic then JOI cleanup models. Because there are three different options for when the JOI cleanup maneuver is performed, three different Monte Carlo simulations are performed for both the GJ and the IJ single-satellite-aided capture trajectories. Data involving the flyby, maneuver, and capture orbit characteristics are collected for each of the many runs in each of the 6 Monte Carlo simulations. This single-satellite-aided capture navigation model is termed the "ballistic then JOI cleanup" model.

The first Monte Carlo model for the double-satellite-aided captures is similar to that of the single-satellite-aided captures and is also termed the "ballistic then JOI cleanup" model. The errors on both flybys are found by multiplying the state transition matrices (from the initial state to the state at each flyby) by the initial state errors. The state error before the JOI maneuver is found similarly, and the JOI maneuver is perturbed via the Cassini MEA maneuver model. A JOI cleanup maneuver is performed 1, 2, or 3 days later and the apojove velocity mismatch is considered to be another maneuver. Since there are three nominal double-satellite-aided capture sequences (GIJ, GEJ, and CGJ) and three different JOI cleanup maneuver times for each of them, there are 9 different Monte Carlo simulations.

TCM and JOI re-target model. The second Monte Carlo model for the double-satellite-aided captures is termed the "TCM and JOI re-target" model. The spacecraft is propagated to the first flyby and its error is modeled using the state transition matrix. The spacecraft is then propagated to a time 6 hours after the first flyby, where its receives a knowledge update and performs a TCM. The knowledge update is modeled by calculating (via state transition matrix propagation) and adding the errors at the time of the TCM to the nominal trajectory. The nominal TCM is calculated by targeting the nominal B-plane of the second flyby. Once the nominal TCM is calculated, the JOI maneuver is also re-targeted to match the nominal semi-major axis of the capture orbit using the knowledge available from after the first flyby. These calculations are generated deterministically, so they are separate from the Monte Carlo run results.

After the calculations of the TCM and retargeted-JOI maneuver, the Monte Carlo run goes back to the trajectory's state immediately before the TCM. The TCM is perturbed by its maneuver error and executed, and the trajectory is propagated to its second flyby. The second flyby's error is calculated by multiplying the state transition matrix (from the maneuver time to the time of the second flyby) by the smaller knowledge error at the maneuver time (given by column 2 in Table 4). The spacecraft is propagated to perijove, the propagation and maneuver errors are applied to the re-targeted JOI. Like the "ballistic then JOI" cases, a JOI cleanup maneuver is added 1, 2, or 3 days later. Consequently, there are 9 different Monte Carlo simulations for the "TCM and JOI re-target" model also.

RESULTS

Twenty-four different scenarios were run in the Monte Carlo simulation. The Monte Carlo simulation code was slow, so overnight and over-weekend runs were needed to collect enough data

Table 6. Number of Monte Carlo runs for each double- and single-satellite-aided capture scenario.

JOI cleanup (time after JOI)	1 day	2 days	3 days
IJ Ballistic then cleanup	3161	764	856
GJ Ballistic then cleanup	715	734	6412
GIJ Ballistic then cleanup	3015	5427	1468
GIJ TCM and JOI re-target	1591	2725	1650
GEJ Ballistic then cleanup	2954	2991	2972
GEJ TCM and JOI re-target	452	581	579
CGJ Ballistic then cleanup	770	640	2746
CGJ TCM and JOI re-target	482	611	601

for each of the 24 runs. Also, bugs in the Monte Carlo code were found that required many runs to be re-done. Thus, the number of Monte Carlo runs is uneven between scenarios. The "ballistic then JOI cleanup" double-satellite-aided capture sequences had the greatest variability, so they were generally prioritized in terms of ensuring that more Monte Carlo runs were performed for those scenarios. Table 6 lists how many Monte Carlo runs were used for each scenario (the more runs, the better the statistics).

B-plane and Altitude Dispersions

The most important results are the B-plane (and altitude) dispersions of the final flybys of the "ballistic then JOI cleanup" double-satellite-aided captures since they are the only scenarios that pose legitimate risks of collision with the moons. Since the flyby B-plane dispersions are independent of whether the JOI cleanup maneuvers are 1, 2, or 3 days after the JOI maneuver, the B-plane data for the three JOI cleanup maneuver options are combined into single data sets for GIJ, GEJ, and CGJ doubles. The B-plane dispersion results are plotted in Figs. 1, 2, and 3. Each Monte Carlo run is plotted as a blue diamond, the thick black lines represent the 1σ and 3σ error ellipses, and the thin black line represents the surface of each moon. There were no collisions or near collisions for the GIJ and GEJ cases, so the effective collision probability approaches zero for those cases. There were 11 collisions and several near collisions for the CGJ case (out of 4156 runs), so its collision probability is approximately 0.265%.

Altitude statistics for the first (or only) and second flybys of all the single- and double-satellite-aided capture sequences are given for all 8 scenarios in Table 7. Again, the JOI cleanup maneuver time has no effect on these statistics, so the data sets are combined. The B-plane statistics are less intuitive—the B-plane ellipses are all approximately circles, so the standard deviations of the altitudes are similar in magnitude to the standard deviations of both the $\vec{B} \bullet \hat{T}$ and $\vec{B} \bullet \hat{R}$ components. The mean $\vec{B} \bullet \hat{T}$ and $\vec{B} \bullet \hat{R}$ values are consistent with incoming, equatorial, energy-reducing flybys, so the $\vec{B} \bullet \hat{T}$ is positive and slightly higher than the radius of periapsis of the flyby and the $\vec{B} \bullet \hat{R}$ is approximately zero.

Statistical delta-v results

The second most important results of the Monte Carlo simulations were the ΔV values. Table 8 lists the Monte Carlo statistics of the ΔV values for each of the 24 scenarios. The minimum ΔV

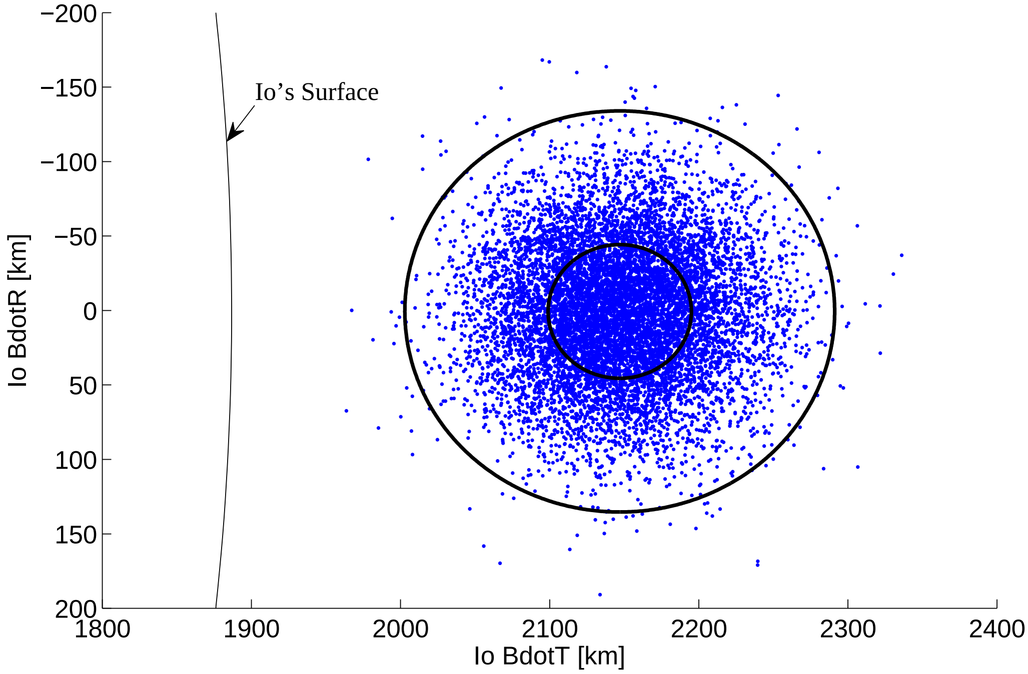

Figure 1. The B-plane dispersions of the second flyby (of Io) of the GIJ capture. There were no collisions with Io in the 9910 Monte Carlo simulations.

Table 7. Altitude statistics for the flybys of all investigated capture strategies. GIJ 1 implies the first flyby (of Ganymede) of the GIJ sequence whereas GIJ 2 implies the second flyby (of Io) of the GIJ sequence.

Altitude statistics (km)	Mean	St. Dev.	Min	1%	Median	99%	Max
IJ Ballistic then cleanup	957.7	5.65	934.1	944.7	957.7	970.6	978.9
GJ Ballistic then cleanup	502.2	5.54	481.1	489.1	502.2	515.1	519.1
GIJ 1 Ballistic then cleanup	141.6	5.65	120.0	128.7	141.5	155.0	164.0
GIJ 2 Ballistic then cleanup	261.1	48.0	81.9	152.0	260.3	375.0	452.3
GIJ 1 TCM and JOI re-target	141.5	5.62	121.3	128.3	141.5	154.9	162.6
GIJ 2 TCM and JOI re-target	254.5	5.21	231.6	242.8	254.4	266.8	272.6
GEJ 1 Ballistic then cleanup	119.0	5.64	96.5	106.1	118.9	132.0	139.5
GEJ 2 Ballistic then cleanup	276.0	58.1	39.6	143.5	275.2	410.2	483.1
GEJ 1 TCM and JOI re-target	119.1	5.63	98.8	105.3	119.2	133.3	141.1
GEJ 2 TCM and JOI re-target	234.9	4.96	219.8	223.6	234.9	246.4	251.8
CGJ 1 Ballistic then cleanup	96.5	5.70	76.0	82.9	96.6	109.4	116.9
CGJ 2 Ballistic then cleanup	233.2	84.7	-95.6	38.2	232.1	432.5	571.5
CGJ 1 TCM and JOI re-target	96.8	5.65	79.5	83.3	96.7	109.3	114.7
CGJ 2 TCM and JOI re-target	210.9	5.23	194.7	198.9	210.8	223.4	232.5

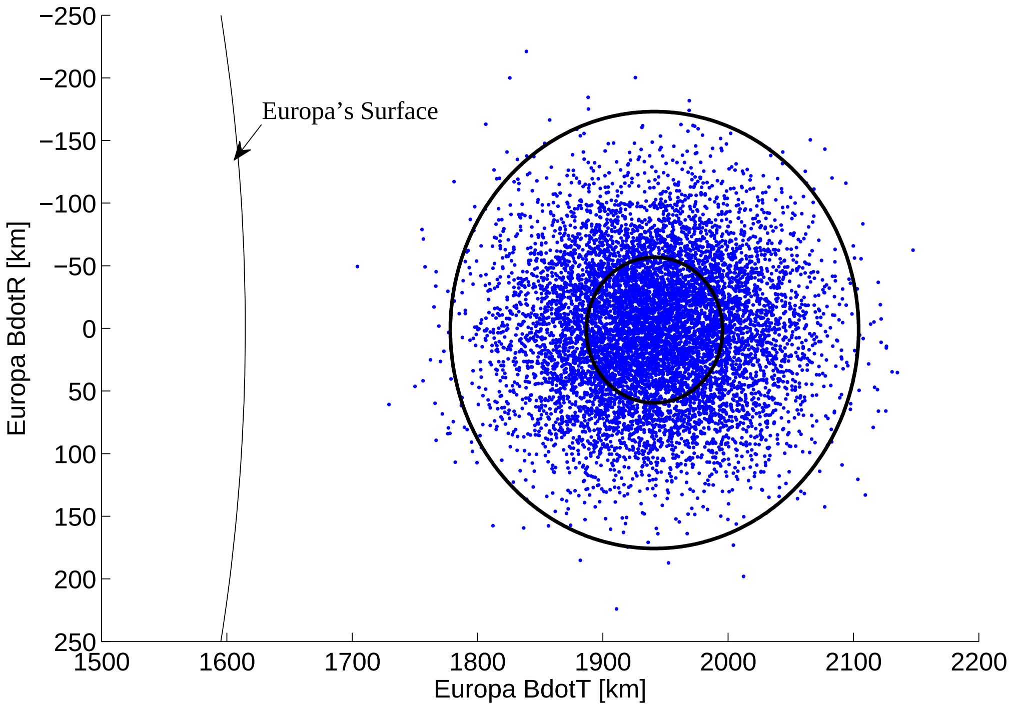

Figure 2. The B-plane dispersions of the second flyby (of Europa) of the GEJ capture. There were no collisions with Europa in the 8917 Monte Carlo simulations.

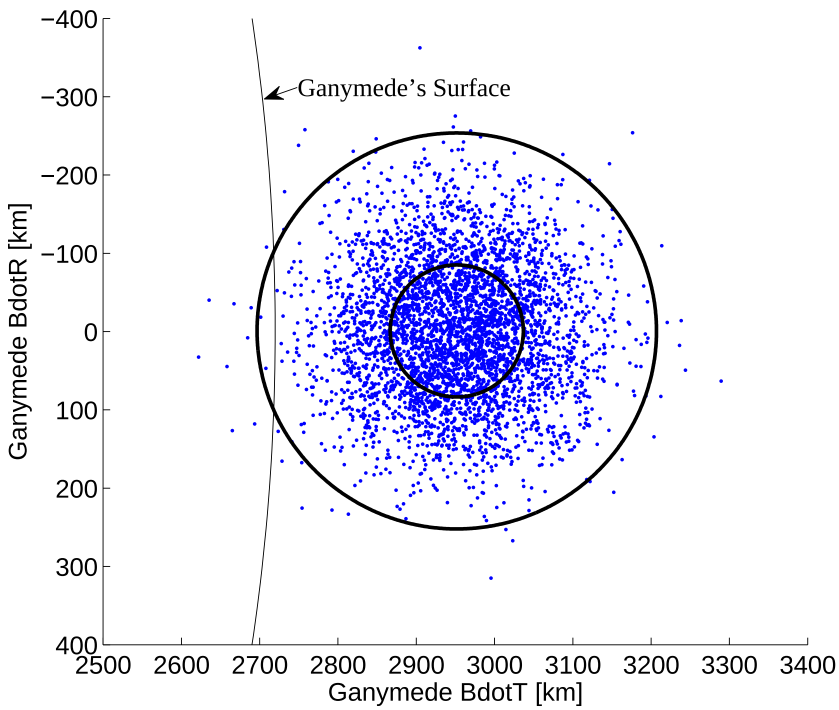

Figure 3. The B-plane dispersions of the second flyby (of Ganymede) of the CGJ capture. There were 11 collisions with Ganymede in the 4156 Monte Carlo simulations. Thus, the collision probability is 0.265% for this particular nominal CGJ capture.

values were close to the deterministic ΔV values for all of the captures, so subtracting the other results from the minima would give a good estimate of the additional statistical ΔV needed to complete the captures. The 99th percentile ΔV is typically used in practice to give an estimate for the ΔV budgets of missions,[37] so that value is more practically important than the absolute maxima of each case. (The absolute maxima are often outliers.)

In general, the single-satellite-aided captures and the "canned TCM and JOI re-target" double-satellite-aided capture sequences have much lower (better) statistical ΔV costs than the "ballistic then JOI cleanup" double-satellite-aided capture sequences. The "ballistic then JOI cleanup" double-satellite-aided capture sequences also have much more extreme values for their 99th percentile and maximum ΔV values. We also note that the 11 collision cases are analyzed as if they did not collide with Ganymede for the purposes of calculating the statistical ΔV.

DISCUSSION

Collision risk mitigation

Since the CGJ "ballistic then JOI cleanup" scenario was the only one that had collisions with a moon (Ganymede), we will first discuss the ramifications of that. Since the collision risk was less than 1% (0.265%), it could be deemed an acceptable risk depending on the risk requirements of the mission. The minimum periapsis altitude of the colliding cases was -95 km, so a similar nominal trajectory could be constructed with the same nominal Callisto flyby altitude, but with a Ganymede flyby altitude that is 100 km or more higher.

Throughout this paper, we assume that the "TCM and JOI re-target" case would be the nominal strategy and the "ballistic then JOI cleanup" would only be a contingency scenario if the "TCM and JOI re-target" case failed. If we combine the operational failure probability of "TCM and JOI re-target" case with the collision probability of the "ballistic then JOI cleanup", then the probability of mission failure would be much lower. The failure risk might then become acceptable. Furthermore, a contingency plan could be added such that the spacecraft would automatically raise the Ganymede flyby altitude if a command from the ground was not received. Although there is some failure risk due to collisions, the CGJ "ballistic then JOI cleanup" scenario is still feasible since there are many ways to mitigate the risk. The same logic would apply to the minor collision risks of the GIJ and GEJ "ballistic then JOI cleanup" scenarios that are below the resolution of the Monte Carlo simulations.

Comparison of statistical delta-v results

The results show that substantial amounts of statistical ΔV can be saved by using double-satellite-aided captures rather than single-satellite-aided captures. The 99th percentile[37] statistical ΔV of the 1 day cleanup cases are used in this comparison, and are tabulated in Table 9. For the "TCM and JOI re-target" cases, the statistical ΔV savings of double- vs. single-satellite-aided capture mirror the deterministic savings in Table 1. The "ballistic then JOI cleanup" cases still save a substantial amount of the statistical ΔV savings vs. single-satellite-aided capture, but the savings are not as dramatic. The perijoves are also listed in Table 9 to provide context.

For missions that consider perijoves below Io's orbit to be acceptable, the three options are IJ, GIJ ballistic then cleanup, and GIJ TCM and JOI re-target. GIJ ballistic then cleanup saves 196.4 m/s vs. IJ, and GIJ TCM and JOI re-target saves 261.2 m/s vs. IJ. To provide context for those savings, we note that the IJ trajectory was based on the JEO study that used an extremely conservative 1000 km altitude Io flyby[31] and the IJ and the GIJ trajectories used different interplanetary trajectories.

Table 8. Statistical ΔV (in m/s) required for all single- and double-satellite-aided capture strategies.

Statistical ΔV (m/s)	Mean	St. Dev.	Min	Median	99%	Max
IJ Ballistic then 1 day cleanup	599.1	2.15	596.0	598.6	606.4	610.7
IJ Ballistic then 2 day cleanup	599.9	2.66	596.1	599.3	608.4	610.6
IJ Ballistic then 3 day cleanup	600.3	2.99	596.1	599.6	609.6	615.2
GJ Ballistic then 1 day cleanup	918.0	2.75	913.6	917.4	926.4	930.8
GJ Ballistic then 2 day cleanup	918.9	3.30	913.8	918.2	928.7	934.4
GJ Ballistic then 3 day cleanup	919.2	3.52	913.6	918.6	929.9	940.5
GIJ Ballistic then 1 day cleanup	360.4	17.0	337.2	356.4	410.0	446.2
GIJ Ballistic then 2 day cleanup	362.1	18.6	337.2	358.2	415.5	456.3
GIJ Ballistic then 3 day cleanup	364.6	20.2	337.1	360.0	422.8	442.3
GIJ TCM and JOI re-target; 1 day	340.6	1.70	337.2	340.4	345.2	347.5
GIJ TCM and JOI re-target; 2 day	340.5	1.79	337.2	340.2	345.8	348.0
GIJ TCM and JOI re-target; 3 day	340.5	1.80	337.3	340.2	345.8	348.6
GEJ Ballistic then 1 day cleanup	709.5	20.2	681.7	705.2	767.4	800.1
GEJ Ballistic then 2 day cleanup	712.3	22.1	681.7	708.4	773.2	799.0
GEJ Ballistic then 3 day cleanup	714.4	23.8	681.8	709.9	782.6	811.3
GEJ TCM and JOI re-target; 1 day	687.0	2.09	682.4	686.9	692.5	695.9
GEJ TCM and JOI re-target; 2 day	687.0	2.27	682.7	686.8	694.0	696.5
GEJ TCM and JOI re-target; 3 day	687.1	2.26	682.5	686.8	693.3	696.3
CGJ Ballistic then 1 day cleanup	639.8	29.1	600.1	631.7	728.2	798.4
CGJ Ballistic then 2 day cleanup	639.3	27.7	597.4	634.9	718.7	770.2
CGJ Ballistic then 3 day cleanup	641.7	31.6	597.5	634.7	737.2	790.3
CGJ TCM and JOI re-target; 1 day	601.8	2.08	597.6	601.5	608.3	611.1
CGJ TCM and JOI re-target; 2 day	601.7	1.99	597.8	601.3	607.4	609.1
CGJ TCM and JOI re-target; 3 day	602.0	2.35	597.8	601.5	608.4	613.5

Table 9. Perijove and 99th percentile statistical ΔV comparisons for each of the scenarios. The scenarios with 1 day JOI cleanup maneuvers are used.

Scenario	Nominal Rp (R_{J})	ΔV_{99} (m/s)
IJ Ballistic then cleanup	5.07	606.4
GJ Ballistic then cleanup	12.1	926.4
GIJ Ballistic then cleanup	5.44	410.0
GIJ TCM and JOI re-target	5.44	345.2
GEJ Ballistic then cleanup	8.69	767.4
GEJ TCM and JOI re-target	8.69	692.5
CGJ Ballistic then cleanup	8.57	728.2
CGJ TCM and JOI re-target	8.57	608.3

A more thorough comparison from a holistic mission architecture perspective is beyond the scope of this paper.

The comparison between the GJ and the four GEJ and CGJ cases is even less straightforward since their perijoves are different. About 100 m/s of perijove raise maneuver ΔV would be required to raise the second perijoves of the GEJ and CGJ cases to the second perijove of the GJ capture.[38] However, the need to raise perijove is related to radiation concerns, which may or may not be as important as saving ΔV (depending on the mission architecture). Additionally, the GJ sequence was based on the nominal Europa mission[32] and had a conservative 500 km flyby of Ganymede and a different interplanetary trajectory from the other cases. For the purposes of this comparison, we will just take the statistical ΔV numbers as they are in Table 9. The GEJ ballistic then cleanup, GEJ TCM and JOI re-target, CGJ ballistic then cleanup, and CGJ TCM and JOI re-target cases save 159.0, 233.9, 198.2, and 318.1 m/s, respectively, compared to the GJ case.

Operations

Since the Galileo mission[11,12] successfully used an IJ sequence to capture into Jupiter orbit, single-satellite-aided capture has operational heritage and is clearly feasible. Double flybys have been used several times by the Cassini mission,[39,39] so the navigation of those Cassini double flybys will now be compared with the double-satellite-aided capture sequences in this paper. The Cassini double flybys occurred many years into the satellite tour rather than as part of the capture sequence, so the ephemerides of the Saturnian moons were extremely good compared to our ephemeris knowledge of the Galilean moons. Cassini did not have a large JOI maneuver to execute after the double flybys, it did not use canned maneuvers in-between flybys, and only one of the moons (Titan) had a comparable amount of gravity to the Galilean moons.

All of the Cassini double flybys used a “ballistic then flyby cleanup” strategy, but they did not have the collision risks or large statistical ΔV costs that are associated with the “ballistic then JOI cleanup” double-satellite-aided capture sequences in this paper. However, the navigation of the “ballistic then JOI cleanup” double-satellite-aided capture strategies in this paper is qualitatively similar enough to the Cassini double flybys that the “ballistic then JOI cleanup” double-satellite-aided capture sequences could be considered to have *de facto* operational heritage.

The “TCM and JOI re-target” scenarios do not have any direct operational heritage, but all the required elements of the strategy have substantial operational heritage. The GIJ, GEJ, and CGJ nominal trajectories have about 14.5, 12.5, and 21.5 hours in between flybys, respectively. The one-way light time delay between Earth and Jupiter varies between about 35 minutes and 50 minutes. In our model, we assume that the TCMs occur 6 hours after the first flyby. Although operational cycles for navigating satellite flybys are usually on the order of 1-3 days, six hours is enough time to get a sufficiently precise radiometric navigation solution, to re-target the canned TCM and JOI maneuvers, and to send the instructions from Earth to Jupiter.

CONCLUSIONS

Prior work had demonstrated that substantial deterministic ΔV savings are available by using double-satellite-aided captures rather than single-satellite-aided captures. However, a full statistical ΔV analysis had not been performed. This paper demonstrates that substantial statistical ΔV savings are still available using standard radiometric navigation techniques. While one of the cases has a small (0.265%) collision risk, all the other cases do not have any detectable collision risk within the resolution of the Monte Carlo simulation. The results of this analysis provide further evidence for the viability and utility of double-satellite-aided capture sequences for future missions to Jupiter such as NASA's Europa Mission and ESA's JUICE mission.

REFERENCES

[1] R. W. Longman, "Gravity Assist from Jupiter's Moons for Jupiter-Orbiting Space Missions," tech. rep., The RAND Corp., Santa Monica, CA, 1968.

[2] R. W. Longman and A. M. Schneider, "Use of Jupiter's Moons for Gravity Assist," *Journal of Spacecraft and Rockets*, Vol. 7, No. 5, May 1970, pp. 570–576.

[3] J. K. Cline, "Satellite Aided Capture," *Celestial Mechanics*, Vol. 19, May 1979, pp. 405–415.

[4] K. T. Nock and C. Uphoff, "Satellite Aided Orbit Capture," *AAS Paper 79-165, Proceedings of the AAS/AIAA Astrodynamics Specialist Conference*, Provincetown, MA, June 25–27, 1979.

[5] M. Malcolm and C. McInnes, "Spacecraft Planetary Capture Using Gravity-Assist Maneuvers," *Journal of Guidance, Control, and Dynamics*, Vol. 28, March-April 2005, pp. 365–368.

[6] C. H. Yam, *Design of Missions to the Outer Planets and Optimization of Low-Thrust, Gravity-Assist Trajectories via Reduced Parameterization*. PhD thesis, School of Aeronautics and Astronautics, Purdue University, West Lafayette, IN, May 2008, pp. 96–104.

[7] J. D. Anderson, R. A. Jacobson, T. P. McElrath, W. B. Moore, G. Schubert, and P. C. Thomas, "Shape, Mean Radius, Gravity Field, and Interior Structure of Callisto," *Icarus*, No. 153, 2001.

[8] J. D. Anderson, E. L. Lau, W. L. Sjogren, G. Schubert, and W. B. Moore, "Gravitational Constraints on the Internal Structure of Ganymede," *Nature*, No. 384, December 1996, pp. 541–543.

[9] J. D. Anderson, G. Schubert, R. A. Jacobson, E. L. Lau, W. B. Moore, and W. L. Sjogren, "Europa's Differentiated Internal Structure: Inferences from Four Galileo Encounters," *Science*, No. 281, 1998.

[10] J. D. Anderson, R. A. Jacobson, E. L. Lau, W. B. Moore, and G. Schubert, "Io's Gravity Field and interior Structure," *Journal of Geophysical Research*, No. 106, 2001.

[11] C. Potts and M. Wilson, "Maneuver Design for the Galileo VEEGA Trajectory," *AAS Paper 93-566, Proceedings of the AAS/AIAA Astrodynamics Specialist Conference*, Victoria, B.C., Canada, Aug. 1993.

[12] T. Barber, F. Krug, and B. Froidevaux, "Initial Galileo Propulsion System In-Flight Characterization," *AIAA Paper No: 93-2117, Proceedings of the AIAA/SAE/ASME/ASEE 29th Joint Propulsion Conference and Exhibit*, Monterrey, CA, June 1993.

[13] J. R. Johannesen and L. A. D'Amario, "Europa Orbiter Mission Trajectory Design," *AAS Paper 99-330, Proceedings of the AAS/AIAA Astrodynamics Conference*, Vol. 103, Girdwood, AK, August 1999.

[14] D. Landau, N. Strange, and T. Lam, "Solar Electric Propulsion with Satellite Flyby for Jovian Capture," *Proceedings of the AAS/AIAA Spaceflight Mechanics Conference*, San Diego, CA, February 2010.

[15] A. E. Lynam, K. W. Kloster, and J. M. Longuski, "Multiple-satellite-aided Capture Trajectories at Jupiter using the Laplace Resonance," *Celestial Mechanics and Dynamical Astronomy*, Vol. 109, No. 1, 2011.

[16] A. E. Lynam and J. M. Longuski, "Interplanetary Trajectories for Multiple Satellite-Aided Capture at Jupiter," *Journal of Guidance, Control, and Dynamics*, Vol. 34, No. 5, September-October 2011.

[17] N. Strange, D. Landau, R. Hofer, J. Snyder, T. Randolph, S. Campagnola, J. Szabo, and B. Pote, "Solar Electric Propulsion Gravity-Assist Tours For Jupiter Missions," *AIAA Paper No: 2012-4518, Proceedings of the AIAA/AAS Astrodynamics Specialists Conference*, Minneapolis, MN, August 2012.

[18] D. Izzo, L. F. Simões, M. Märtens, G. C. H. E. d. Croon, A. Heritier, and C. H. Yam, "Search for a Grand Tour of the Jupiter Galilean Moons," *Proceedings of the 15th Annual Conference on Genetic and Evolutionary Computation*, Amsterdam, The Netherlands, July 2013.

[19] M. Schadegg, R. P. Russell, and G. Lantoine, "Jovian Orbit Capture and Eccentricity Reduction Using Electrodynamic Tether Propulsion," *Journal of Spacecraft and Rockets*, Vol. 52, 2015.

[20] A. E. Lynam, "Broad-Search Algorithms for Finding Triple- and Quadruple-Satellite-Aided Captures at Jupiter from 2020 to 2080," *Celestial Mechanics and Dynamical Astronomy*, Vol. 121, 2015.

[21] A. E. Lynam, "Broad-search Algorithms for the Spacecraft Trajectory Design of Callisto-Ganymede-Io triple flybys from 2024-2040, Part I: Heuristic Pruning of the Solution Space," *Acta Astronautica*, Vol. 94, 2014.

[22] A. E. Lynam, "Broad-search Algorithms for the Spacecraft Trajectory Design of Callisto-Ganymede-Io triple flybys from 2024-2040, Part II: Lambert Pathfinding and Trajectory Solutions," *Acta Astronautica*, Vol. 94, 2014.

[23] A. M. Didion and A. E. Lynam, "Impulsive Trajectories from Earth to Callisto-Io-Ganymede Triple Flyby Capture at Jupiter," *Journal of Spacecraft and Rockets*, Vol. 52, 2015.

[24] S. K. Patrick and A. E. Lynam, "Optimal SEP Trajectories from Earth to Jupiter with Triple Flyby Capture," *AIAA Paper No: 2014-4218, AIAA/AAS Astrodynamics Specialist Conference*, San Diego, CA, August 2014.

[25] S. K. Patrick and A. E. Lynam, "High-fidelity Low-thrust SEP trajectories from Earth to Jupiter Capture," *AAS Paper No 15-609, AAS/AIAA Astrodynamics Specialist Conference*, Vail, CO, August 2015.

[26] B. M. Portock, R. Haw, and L. A. D'Amario, "2003 Mars Exploration Rover Orbit Determination using Delta-VLBI Data," *AIAA Paper 02-0262, AIAA/AAS Astrodynamics Specialist Conference*, Monterey, CA, August 2002.

[27] D. Roth, P. Antreasian, J. Bordi, K. Criddle, R. Ionasescu, R. Jacobson, J. Jones, M. C. Meed, I. Roundhill, and J. Stauch, "Cassini Orbit Reconstruction from Jupiter to Saturn," *AAS Paper 05-311, Proceedings of the AAS/AIAA Astrodynamics Specialist Conference*, Lake Tahoe, CA, August 2005.

[28] A. E. Lynam and J. M. Longuski, "Preliminary Analysis for the Navigation of Multiple-satellite-aided Capture Sequences at Jupiter," *Acta Astronautica*, 2012.

[29] A. M. Didion and A. E. Lynam, "Guidance and Navigation of a Callisto-Io-Ganymede Triple Flyby Jovian Capture," *AAS Paper No 15-624, AAS/AIAA Astrodynamics Specialist Conference*, Vail, CO, August 2015.

[30] A. Lynam, "Broad Search for Direct Trajectories from Earth to Double-satellite-aided Capture at Jupiter with Deep Space Maneuvers," *AAS Paper No 16-227, AAS/AIAA Spaceflight Mechanics Meeting*, Napa Valley, CA, February 2016.

[31] K. W. Kloster, A. E. Petropoulos, and J. M. Longuski, "Europa Orbiter Mission Design with Io Gravity Assists," *Acta Astronautica*, Vol. 68, 2011.

[32] T. Lam, J. J. Arrieta-Camacho, and B. B. Buffington, "The Europa Mission: Multiple Europa Flyby Trajectory Design Trades and Challenges," *AAS Paper No 15-657, AAS/AIAA Astrodynamics Specialist Conference*, Vail, CO, August 2015.

[33] D. W. Curkendall and J. S. Border, "Delta-DOR: The One-Nanoradian Navigation Measurement System of the Deep Space Network—History, Architecture, and Componentry," *The Interplanetary Network Progress Report*, Vol. 42-193, 2013.

[34] R. Jacobson, R. Haw, T. McElrath, and P. Antreasian, "A Comprehensive Orbit Reconstruction for the Galileo Prime Mission in the J2000 System," *AAS Paper No 99-330, AAS/AIAA Astrodynamics Specialist Conference*, Girdwood, AK, August 1999.

[35] S. V. Wagner and T. D. Goodson, "Execution-Error Modeling and Analysis of the Cassini-Huygens Spacecraft through 2007," *AAS Paper 08-113, Proceedings of the AAS/AIAA Space Flight Mechanics Meeting*, Galveston, TX, January 2008.

[36] C. R. Gates, "A Simplified Model of Midcourse Maneuver Execution Errors," tech. rep., Jet Propulsion Laboratory, Pasadena, CA, 1963.

[37] B. B. Buffington, "Trajectory Design for the Europa Clipper Mission Concept," *AIAA No 2014-4105, AIAA/AAS Astrodynamics Specialist Conference*, San Diego, CA, August 2014.

[38] A. E. Lynam, “Broad Search for Trajectories from Earth to Callisto-Ganymede-JOI Double-satellite-aided Capture at Jupiter from 2020 to 2060,” *Celestial Mechanics and Dynamical Astronomy*, 2015.

[39] J. Arrieta, C. G. Ballard, and Y. Hahn, “Cassini Solstice Mission Maneuver Experience: Year Two,” *Proceedings of the AIAA/AAS Astrodynamics Conference*, Minneapolis, MN, August 2012.